*International Journal of Infrared and Millimeter Waves, Vol. 21, No. 3, 2000*

# VISIBLE LIGHT EMISSION DUE TO RESONANT $CO_2$ LASER EXCITATION OF DENTAL HARD TISSUE

**A. Lohner,[1] M. Huber,[1,2] S. D. Ganichev,[1] W. Prettl,[1] and H. Niederdellmann[2]**

[1]*Institut für Experimentelle und Angewandte Physik*
*Universität Regensburg*
*93040 Regensburg, Germany*
[2]*Klinik und Poliklinik für Mund-, Kiefer- und Gesichtschirurgie*
*Universität Regensburg*
*93040 Regensburg, Germany*

Received December 3, 1999

## Abstract

Visible light emission of dental hard substances excited by high-power infrared pulses of a tunable TEA $CO_2$ laser has been investigated. A clear correlation between observed visible light emission, plasma formation as well as ablation of dental hard tissue has been demonstrated. Both, the highly nonlinear infrared to visible upconversion process and the ablation efficiency show a sharp spectral resonance close to a vibrational mode of $PO_4$ at 1090 $cm^{-1}$ in dental enamel and dentin. The influence of strong infrared light impulses on dental hard tissue is examined by performing upconversion studies of visible light emission of human dental enamel and dentin. Our experimental setup allows one to determine the plasma formation threshold being important in dental surgery.

**Key words:** $CO_2$ laser; hydroxyapatite; infrared absorption; laser ablation; plasma threshold; $PO_4$ mode; upconversion.



0195-9271/00/0300-0407$18.00/0 

# 1 Introduction

Numerous studies have shown that $CO_2$ lasers can be used to modify the surface morphology of dental hard tissue [1–3]. Especially short pulse $CO_2$ laser can efficiently ablate dental hard tissue. Application of the transversaly excited atmospheric pressure (TEA) $CO_2$ laser has demonstrated that surface changes and ablation of dental enamel can be produced which have a strong wavelength dependence [1, 4, 5]. These effects of the $CO_2$ laser on the tissue have recently been studied with scanning electron microscopy (SEM) and were attributed to the strong phosphate and carbonate absorption bands in dental enamel [1]. These studies were carried out with the strong $CO_2$ laser lines at wavelengths at 9.3 $\mu$m, 9.6 $\mu$m and 10.6 $\mu$m. The observed surface effects at 9.3 $\mu$m were much more efficient than at the 10.6 $\mu$m wavelength.

Ablation of dental hard tissue has also been reported using other laser systems. Investigation performed with a picosecond Nd: YLF oscillator laser with a emission wavelength of 1.053 $\mu$m has reported plasma-induced ablation when exceeding the threshold of optical breakdown. A visible plasma spark could be observed for excitation densities $\geq 10^{12}$ W/cm$^2$ [6].

Effective use of lasers for dental treatments requires accurate knowledge of the physical processes which leads to the absorption of laser energy deposited during irradiation. The optimal excitation parameter like excitation wavelength, energy density, pulse duration and repetition rate have to be determined.

In this work, we report on a study of visible light emission of dental enamel excited by a pulsed $CO_2$ laser with intensities well below the plasma formation threshold. As has been shown previously upconversion from the spectral range of $CO_2$ laser radiation into the visible occurs in dental enamel [7] very similar to upconversion observed in porous silicon [8, 9]. Visible radiation is only observed at a narrow band of excitation in the infrared which can be related to vibrational modes of phosphate ions in dental enamel. The emission in the visible range is a highly nonlinear function of the infrared excitation intensity $I_{IR}$. Temporally resolved luminescence and luminescence excitation spectra have been measured giving insight into the absorption processes which result in the emission of light. Two contributions to the overall light emission with complete different spectral and temporal characteristics can be identified.

# 2 Experimental

In our experiments, planparallel thin sections (about 1-2 mm thick) from extracted human teeth are mounted in a chamber evacuated to 1 mbar. Single high-power IR pulses of a TEA $CO_2$ gas laser tunable in discrete steps from 926 to 1088 $cm^{-1}$ (9.2 - 10.8 $\mu$m) serve as radiation sources of the teeth. The pulse width is 150 ns in the primary peak, followed by a low intensity tail of about 1 $\mu$s. The pulse power of the incident IR pulses was controlled by inserting calibrated $CaF_2$ absorbers and simultaneously monitored by means of a calibrated fast photon drag detector [10]. A thick Ge window is used as a cut-off filter to suppress visible light in the excitation pulse. The luminescence of the teeth are spectrally and temporally resolved using a monochromator and a photomultiplier with a time resolution of 5 ns. The photoluminescence spectra are corrected for the spectral response of the optical system. The peak excitation intensities of a laser pulse given below are determined from the spot size of the laser beam on the sample and the maximum of the photon-drag detector signal.

# 3 Experimental Results

We observe visible luminescence up to photon energies of 2.8 eV. The luminescence signal occurs only in a very narrow band of infrared excitation around 1088 $cm^{-1}$. In Fig. 1 we present time resolved measurements of the light emission of dentin at a photon energy $E_{LUM}$ = 2.58 eV for excitation intensities $I_{IR}$ from 10 to 29 MW/$cm^2$. We observe two components separated in time. The amplitude of the early component has its maximum after a fast rise at $\tau$ = 0.3 $\mu$s and decays on a nanosecond timescale. The second peak reaches its maximal value at 1.5 $\mu$s and follows a mono-exponential decay. The time constants exhibits an increase with increasing IR excitation intensity from 1 $\mu$s at 10 MW/$cm^2$ to 3 $\mu$s at 29 MW/$cm^2$. The two components of light emission show a different dependence on excitation intensity $I_{IR}$. For intensities $I_{IR} \leq 16$ MW/$cm^2$ the second peak (peak 2, see Fig. 1) dominates the signal. With increasing IR intensities, the contribution of peak 2 is reduced in comparison to the fast component at early times (peak 1) and a visible plume can be observed pointing towards the laser source. At high intensities the fast peak 1 is substantially higher than any other visible emission. It can uniquely be attributed to the shining plasma plume. This plume is generated, as the amplitude of the electric field exceeds the threshold

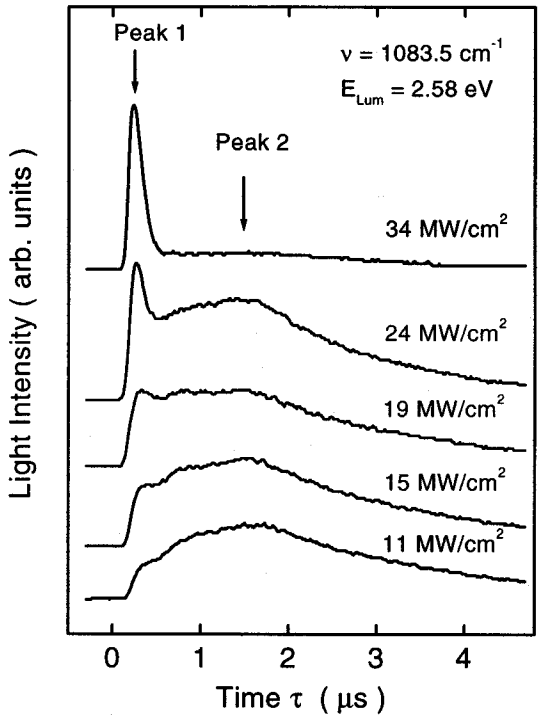


Figure 1: *Temporal kinetics of light emission of dentin after pulsed $CO_2$ laser excitation. Light emission intensity after IR excitation at $\nu = 1083.5\ cm^{-1}$ is plotted for various excitation intensities $I_{IR}$. The detection energy was $E_{LUM} = 2.58\ eV$. As only the decay profile is of interest, the curve have been normalized to approximately the same height.*

for plasma formation, thereby initiating an optical breakdown [11]. In the case when plasma sparking occurs, removal of dental substance is observed. This ablation process is called plasma-induced ablation [6]. We would like to point out that in our experiments the threshold for optical breakdown is much lower than reported in previous investigations of the application of high power lasers on teeth [6]. The time resolved studies indicate, that the luminescence observed for laser intensities below plasma formation results from the delayed component. Here no significant surface changes have been observed on the sample.

The strong dependence of the induced light emission on the IR laser intensity is illustrated in Fig. 2 for peak 1 (circles) and peak 2 (squares). The maximal values of each of the temporal components

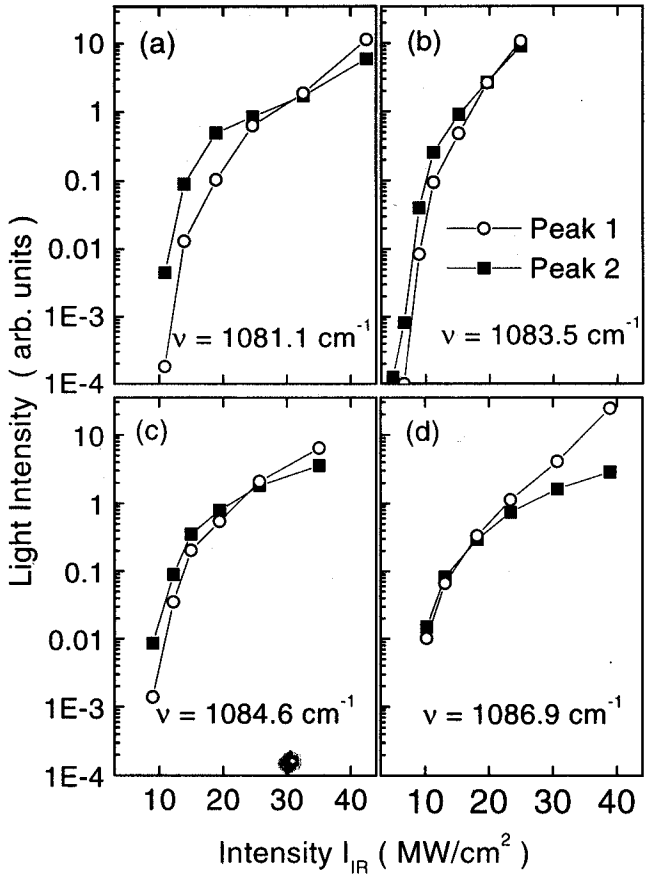


Figure 2: *Magnitude of the emitted light of peak 1 and peak 2 for different $CO_2$ laser excitation energies is plotted vs the excitation intensity $I_{IR}$ of the $CO_2$ laser.*

are plotted logarithmically versus the excitation intensity $I_{IR}$ for four $CO_2$ laser frequencies $\nu$ (Fig. 2(a)-(d)). Both components rise nonlinearly with excitation intensity. A change of the excitation intensity of, for example, a factor of three results in an increase of the emitted light intensity up to four orders of magnitude.

The data in Fig. 2 show again the different intensity dependence of peak 1 and peak 2. At a photon energy of $\nu = 1081.1$ $cm^{-1}$ (Fig. 2a) of the $CO_2$ laser, excitation at intensities below 25 $MW/cm^2$ results in a dominance of peak 2. At higher excitation intensities both components cross each other and the ratio of the

height of peak 1 to peak 2 is inverted. The crossing point of both temporal components shifts to smaller excitation intensities with increasing photon energy of the exciting $CO_2$ laser. This means, that the fast component (peak 1) dominates already at lower excitation intensities. At an excitation energy of the CO2 laser of $\nu = 1084.6$ $cm^{-1}$ (Fig. 2d) peak 1 is larger than peak 2 in the whole observed intensity range.

More specific information on the origin of the excitation process that leads to the light emission is gained from the luminescence-excitation spectrum shown in Fig. 3. The time integrated emission intensity at $E_{LUM} = 2.58$ eV is plotted versus the frequency $\nu$ of the infrared excitation by scanning the lines of the $CO_2$ laser. The measurement shows that there is no light emission for frequencies below 1058 $cm^{-1}$. A pronounced narrow resonance occurs at $\nu = 1083.5$ $cm^{-1}$. The visible emission intensity measured with this laser line is more than ten times stronger than the integrated luminescence intensity of the neighboring laser lines. The rise of the signal at 1088 $cm^{-1}$ indicates a second peak. The structure of this second peak cannot be spectrally measured as no emission lines of our $CO_2$ laser system are accessible for photon energies higher than 1088 $cm^{-1}$.

Dental enamel is a carbonated hydroxyapatite ($Ca_5(PO_4)_3(OH)$) containing 2-5 wt % carbonate, which is crystallographically disordered. The linear infrared spectrum of dental enamel contains bands due to each of the four phosphate internal vibrational modes $\nu_1$-$\nu_4$ and bands corresponding to the four vibrational modes of the carbonate ion and the hydroxyl groups [4]. The intense absorption bands of hydroxyapatite coincide with the TEA $CO_2$ laser lines in the region from $\nu = 929$ $cm^{-1}$ to 1088 $cm^{-1}$.

The arrows in Fig. 3 point to the positions of the infrared active $\nu_3$ vibrational modes of $PO_4$ in the present spectral range as determined from linear absorption measurements [4]. Different frequencies of the $\nu_3$-mode are due to different possible crystallographic sites of $PO_4$ in apatite [4]. The $\nu_3^{(b)}$ mode at 1060 $cm^{-1}$ is not accessible by the $CO_2$ laser due to the gap between the 10 $\mu$m and 9 $\mu$m bands. Specially the intense rise of the visible emission intensity in the IR excitation spectrum (Fig. 3) for frequencies higher than $\nu = 1080$ $cm^{-1}$ coincides with the highest transition frequency of the molecular vibration of the phosphate ion in carbonated hydroxyapatite at $\nu_3^{(a)} = 1090$ $cm^{-1}$. The lack of any luminescence of the $\nu_3^{(c)} = 1032$ $cm^{-1}$ mode might be due that the corresponding crystallographic site is not present in our samples.

As discussed above the two components of the light emission

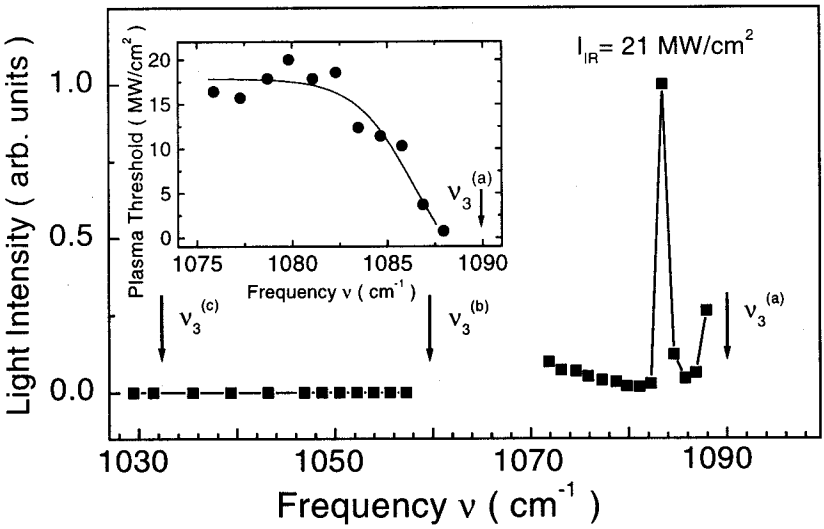


Figure 3: *Light intensity at $E_{LUM}$ = 2.07 eV as a function of the IR frequency $\nu$. The arrows mark the spectral position of the $\nu_3(PO_4)$ transitions. In the range of 1058 cm$^{-1}$ to 1071 cm$^{-1}$ measurements were not possible because of the gap between the two emission bands of the $CO_2$ laser. Inset: Plasma threshold $I_{PL}$ of dentin as a function of the IR frequency $\nu$ as derived from the time resolved measurements. The solid line is to guide the eye.*

show a different time dependence. In order to analyze separately the spectral behavior of the plasma plume (peak 1) and the delayed contribution (peak 2), the visible emission spectrum was measured for different delay times $\tau_D$ after the infrared excitation. The spectral shape of the IR induced luminescence of peak 2 is given in Fig. 4 for two IR excitation intensities at two different frequencies of the $CO_2$ laser. The delay time was set to $\tau_D = 1.5$ $\mu$s. Independently of the chosen excitation conditions a broad structureless luminescence spectra is found for healthy dentin (filled symbols) which shows no wavelength dependence in the observed spectral region and no structures within the resolution of 1 nm. The IR induced luminescence differs substantially from the conventional luminescence of dental enamel after excitation with UV light. There, distinct luminescence peaks are found around 3.5, 3.0, 2.8 and 2.2 eV [12]. The origin of the usual luminescence is presumed to be in the organic and inorganic components of the material.

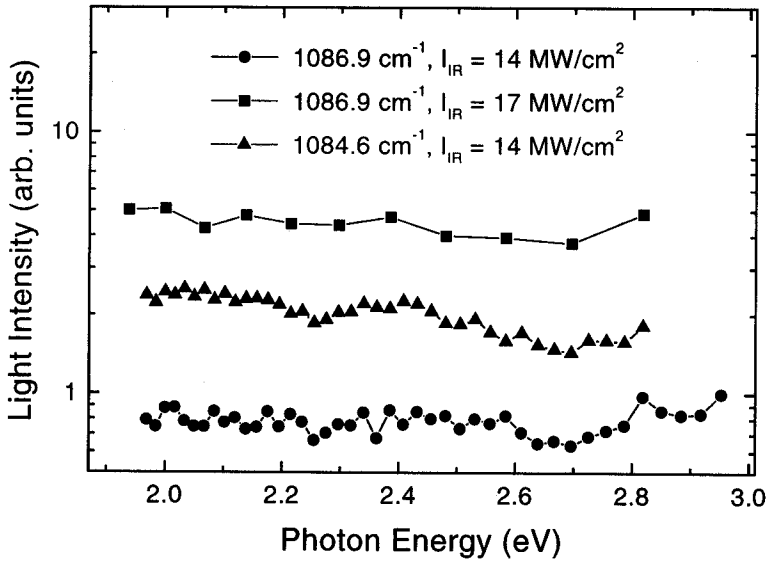


Figure 4: *Spectra of peak 2 after IR excitation at $\nu$ = 1086.9 cm$^{-1}$ and 1084.6 cm$^{-1}$ for two excitation densities ($\tau_D$ = 1.5 $\mu$s).*

In Fig. 5 we present the spectra of the plasma plume for an excitation intensity of 38 MW/cm$^2$ ($\tau_D$ = 0.3 $\mu$s). The light intensity is plotted as a function of the photon energy for an excitation at 1086.9 cm$^{-1}$. While the spectra of the delayed peak exhibited no significant structure, the spectrum of the plasma peak shows several lines which arise from the emission of neutral (Ca) and singly ionized Calcium ($Ca^+$) states [13]. The mineral which shows its strongest emission lines in the observed spectral range occurring in dental hydroxyapatite is Calcium [14]. The lines at 2.847, 2.882 and 2.9337 eV originate from neutral calcium. The signal at 3.0253 eV results probably from singly ionized Calcium. The observed Ca lines were also found by Niemz et al. but using a Nd:YLF laser system at several orders of magnitude higher fluences [6].

In addition, for excitation intensities well above the plasma formation threshold ablation of dental hardsubstances can be observed. The ablation efficiency also changes significantly in the investigated spectral range of the $CO_2$ laser. The most efficient removal of dental substance is achieved for excitation energies very close to the

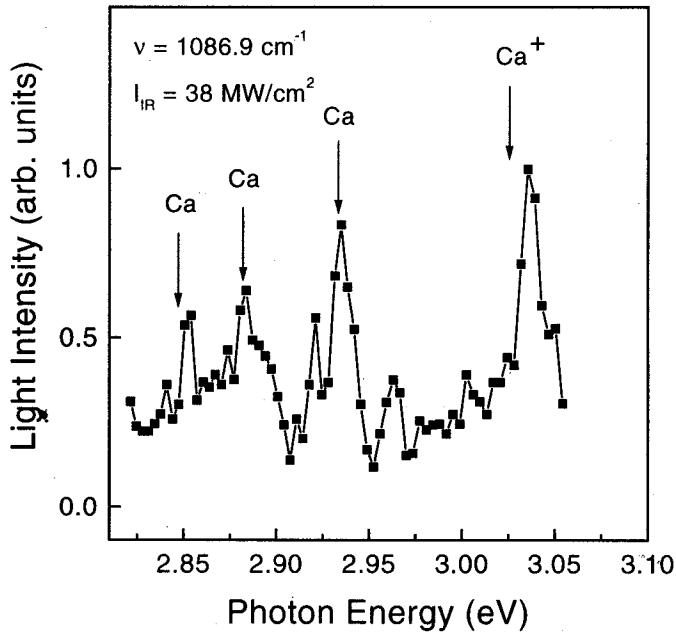


Figure 5: *Spectrum of the IR induced plasma peak (peak 1) for excitation at* $\nu = 1086.9\ cm^{-1}$ ($I_{IR} = 38\ MW/cm^2$, $\tau_D = 1.5\ \mu s$). *The arrows mark the photon energy of the strongest emission lines of neutral and singly ionized Calcium states after [13].*

narrow resonance of the IR induced light emission at 1083.5 $cm^{-1}$ determined in the luminescence excitation spectrum (see Fig. 3).

# 4 Discussion

Different types of physical mechanisms can be considered which might lead to the origin of the enhanced light emission for resonant excitation of dental hardsubstances. The temporally (Fig. 1) and spectrally (Fig. 4 and Fig. 5) resolved data of the IR induced luminescence allow a clear separation of two contributions. The existence of the early component goes hand in hand with the occurrence of a plasma plume as a result of optical breakdown. The high amplitude of the local electric field forces the ionization of molecules

and atoms, starting an electron avalanche process. The following cascade ionization results in a plasma formation [11]. In our experiments the threshold for plasma formation $I_{PL}$ was found to be strongly wavelength dependent. The inset in Fig. 3 illustrates the threshold dependence on excitation energy as determined from the time resolved measurements. For excitation in the frequency range from 1074 to 1088 $cm^{-1}$ where we observe light emission, the values for plasma formation threshold vary between 1 and 25 $MW/cm^2$. In contrast, the threshold for plasma emission determined by Niemz et al. [6] using a Nd:YLF laser at 1.053 $\mu$m with a pulse duration of 30 ps yielding intensities $\geq 5 \times 10^{11}$ $MW/cm^2$. These values lie several orders of magnitude higher compared to ours, even taking into account that the short pulse duration $\tau_{Pulse}$ increases the breakdown threshold, according the relationship $I_{PL} \propto {\tau_{Pulse}}^{x-1}$ [15]. The exponent $x$ is tissue dependent and for pulse durations in the picosecond and nanosecond range, $x$ is found to be 0.46 for dental hardsubstances [15]. According this equation a threshold value of about $9 \times 10^2$ $MW/cm^2$ should be obtained for a pulse duration of $\tau_{Pulse} = 150$ ns. Indeed we observe much lower threshold values. This is due to the significantly higher absorption coefficient of the tooth around 9.3 $\mu$m which lowers the apparent optical breakdown threshold [11]. In contrast, the absorption at 1053 nm is negligible and therefore the threshold is much higher. In this case the plasma formation is induced by the so called dielectric breakdown, as the local electric field exceeds the value of the average intramolecular Coulomb field, thus providing the condition for plasma generation.

In addition the measuered threshold for plasma formation $I_{PL}$ decreases for excitation frequencies close to the resonance frequency of the molecular vibration of the phosphate ion at $\nu_3^{(a)} = 1090$ $cm^{-1}$ (Inset Fig. 3). For an excitation at 1088 $cm^{-1}$ the threshold value was determined to be as small as 1 $MW/cm^2$. We note that the minimum of the plasma formation threshold does not coincide with the peak of the *linear* absorption coefficient ($\approx$ 1030 $cm^{-1}$, [4]). This shows that in the nonlinear process of plasma formation not the strength of absorption is of importance but also the resonance with the $PO_4$ vibrational mode.

In general the initiation of plasma generation in a solid can be two-fold. It was observed that either the free electrons which start an electron avalanche process are generated by thermal laser induced ionization or by laser induced multi-photon ionization [14]. The latter process seems to be responsible for the emission of the plasma plume of dental hardsubstances after intense $CO_2$ laser excitation

because of the strong nonlinear intensity dependence.

The origin of the delayed peak 2 is not yet well understood: Forrer et. al [16] examined the ablation process of bone using a TEA $CO_2$ laser (pulse duration about 1 $\mu$s). They observed a weak light emission even at excitation densities below plasma formation threshold which was attributed without any closer inspection to arise from debris luminescence. But in our case the delayed light emission may not result from glowing of the ejected debris as we observe visible light emission although at excitation densities at which no ablation occurs. Additionally no dependence of the spectral shape on the excitation density is found, as one would expect if thermal processes are involved.

For the medical application determination of the threshold for plasma-formation is very important in several respects:
(1) Electron-microscopic inspection of ablation sites drilled with fluences below and above plasma-formation threshold has shown significantly different histological results. [16] The ablation sites drilled with an intensity below threshold show the natural structure of the hard tissue components. In contrast, for excitation intensities above threshold droplets of solidified melt are observed, indicating thermal damage.
(2) A decrease of ablation efficiency is observed for fluences above plasma formation threshold as the induced plasma absorbs a part of the incident laser radiation, thus screening the tooth surface. [3,16]
(3) Uncontrolled high reflectance of the debris in the plasma plume induced during irradiation represents potential hazards for clinical laser treatment and may be therefore a safety concern. [2]

# 5 Conclusions

In the present study a clear correlation between recently observed visible light emission, plasma formation as well as ablation of dental hard tissue excited by a pulsed high-power $CO_2$ laser has been demonstrated. Both, infrared to visible up-conversion and ablation show a sharp spectral resonance at a vibrational frequency of $PO_4$ in dental enamel and dentin and both processes are highly nonlinear. The plasma threshold has been found to be several orders of magnitude smaller in the resonance than outside. The experimental results suggest that for efficient dental hard tissue treatment the wavelength of short pulsed $CO_2$ lasers should be tuned as close as possible to the spectral position of the $PO_4$ stretch mode at 1090

$cm^{-1}$. Finally it is noted that an analogous resonance in $CO_2$ laser ablation is expected for other hydoxyapatite containing tissue like bones is expected.

# 6 Acknowledgments

Financial support by the Deutsche Forschungsgemeinschaft is gratefully acknowledged.

# References

[1] S. M. McCormack, D. Fried, J. D. B. Featherstone, R. E. Glena, and W. Seka. Scanning Electron Microscope Observations of $CO_2$ Laser Effects on Dental Enamel. J Dent Res 1995; 74: 1702-1708.

[2] D. Fried, R. E. Glena, J. D. B. Featherstone, W. Seka. Permanent and Transient Changes in the Reflectance of $CO_2$ Laser-Irradiated Dental Hard Tissues at $\lambda = 9.3$, 9.6, 10.3, and 10.6 $\mu$m and at Fluences of 1-20 J/cm$^2$. Lasers Surg Med 1997; 20: 22-31.

[3] H. A. Wigdor, J. T. Walsh, J. D. B. Featherstone, S. R. Visuri, D. Fried, J. L. Waldvogel. Lasers in Dentistry. Lasers Surg Med 1995; 16: 103-133.

[4] D. G. A. Nelson and J. D. B. Featherstone. Preparation, Analysis, and Characterization of Carbonated Apatites. Calcif Tissue Int 1982; 34: S69-S81.

[5] G. Duplain, R. Boulay, and P. A. Belanger. Complex index of refraction of dental enamel at $CO_2$ laser wavelength. Appl Opt 1987; 26: 4447-4451.

[6] M. H. Niemz. Investigation and Spectral Analysis of the Plasma-Induced Ablation Mechanism of Dental Hydroxyapatite. Appl Phys B 1994; 58: 273-281.

[7] A. Lohner, S. D. Ganichev, W. M. Huber, J. Diener, W. Prettl. Light Emission of Dental Enamel after Infrared Resonant Excitation. Infrared Phys 1998; 39: 23-28.

[8] J. Diener, M. Ben-Chorin, D. I. Kovalev, S. D. Ganichev and F. Koch. Light from Porous Silicon by Multiphoton Vibronic Excitation. Phys Rev B 1995; 52: R8617-R8620.

[9] J. Diener, S. Ganichev, M. Ben-Chorin, D. Kovalev, V. Petrova-Koch and F. Koch. Quenching and Recovery of the Photoluminescence in Porous Si after Pulse IR Irradiation. Mat Res Soc Symp Proc 1995; 358: 501-506.

[10] A. M. Danishevskiĭ, A. A. Kastal'skiĭ, S. M. Ryvkin, and I. D. Yaroshetskiĭ, Zh Eksp Teor Fiz 1970; 58: 544 [SovPhys JETP 1970; 31: 292].

[11] Y. R. Shen. Infrared Multiphoton Excitation and Dissociation of Molecules. In: Y. R. Shen, ed. *The Principles of Nonlinear Optics.* New York: John Wiley & Sons 1984: 437-465.

[12] D. Spitzer and J. J. ten Bosch. The Total Luminescence of Bovine and Human Dental Enamel. Calcif Tiss Res 1976; 20: 201-208.

[13] J. Reader and C. H Corliss. Line Spectra of the Elements. In: D. R. Lide, H. P. R. Frederikse eds. *Handbook of Chemistry and Physics.* Boca Raton: CRC Press 1993: Cap. 10.

[14] M. H. Niemz. Plasma induced ablation. In: M. H. Niemz, ed. *Laser tissue interactions.* Berlin Heidelberg: Springer-Verlag 1996: 101-123.

[15] M. H. Niemz. Threshold dependence of laser-induced optical breakdown on pulse duration. Appl Phys Lett 1995; 66: 1181-1183.

[16] M. Forrer, M. Frenz, V. Romano, H. J. Altermatt, H. P. Weber, A. Silenok, M. Istomyn, and V. I. Konov. Bone-Ablation Mechanism Using $CO_2$ Lasers of Different Pulse Duration and Wavelength. Appl Phys B 1993; 56: 104-112.